



**AIAA 2004–0029**

**Aero-Structural Wing Planform  
Optimization**

Kasidit Leoviriyakit and Antony Jameson  
*Stanford University, Stanford, CA 94305-4035*

**42<sup>nd</sup> Aerospace Sciences Meeting and Exhibit**  
**January 5–8, 2004**  
**Reno, Nevada**

# AERO-STRUCTURAL WING PLANFORM OPTIMIZATION

Kasidit Leoviriyakit \* and Antony Jameson †  
*Stanford University, Stanford, CA 94305-4035*

During the last decade, aerodynamic shape optimization methods based on control theory have been intensively developed. The methods have proved to be very effective for improving wing section shapes for fixed wing-planforms. Building on this success, extension of the control theory approach to variable planforms has yielded further improvement. This paper describes the formulation of optimization techniques based on control theory for aerodynamic shape design in inviscid compressible flow modeled by the Euler equations. The design methodology has been expanded to include wing planform optimization. It extends the previous work on wing planform optimization based on simple wing weight estimation. A more realistic model for the structural weight, which is sensitive to both planform variations and wing loading, is included in the design cost function to provide a meaningful design. A practical method to combine the structural weight into the design cost function is studied. An extension of a single to a multiple objective cost function is also considered. Results of optimizing a wing-fuselage of a commercial transport aircraft show a successful trade-off between the aerodynamic and structural cost functions, leading to meaningful wing planform designs. The results also support the necessity of including the structural weight in the cost function. Furthermore, by varying the weighting constant in the cost function, an optimal set called “Pareto front” can be captured, broadening the design range of optimal shapes.

## Introduction

WHILE aerodynamic prediction methods based on CFD are now well established, quite accurate, and robust, the ultimate need in the design process is to find the optimum shape which maximizes the aerodynamic performance. One way to approach this objective is to view it as a control problem, in which the wing is treated as a device which controls the flow to produce lift with minimum drag, while meeting other requirements such as low structural weight, sufficient fuel volume, and stability and control constraints. In this paper, we apply the theory of optimal control of systems governed by partial differential equations with boundary control, in this case through changing the shape of the boundary. Using this theory, we can find the Frechet derivative (infinitely dimensional gradient) of the cost function with respect to the shape by solving an adjoint problem, and then we can make an improvement by making a modification in a descent direction. For example, the cost function might be the drag coefficient at a fixed lift, or the lift to drag ratio. During the last decade, this method has been intensively developed, and has proved to be very effective for improving wing section shapes for fixed wing planforms.<sup>1-8</sup> Furthermore, this method is not limited to only the wing sections but can be extended to wing planforms.

Wing planform modification can yield large improvement in wing performance but can also affect wing weight and stability and control issues. It is well known that the induced drag varies inversely with the square of the span. Hence the induced drag can be reduced by increasing the span. Moreover, shock drag in transonic flow might be reduced by increasing sweepback or increasing the chord to reduce the thickness to chord ratio. However, a pure aerodynamic optimization may lead to highly suspect results because the decrease in drag might come at the expense of the increase in wing weight. Therefore it is essential to account for the effect of planform change on wing weight. Also, for practical design purposes, a fast and accurate method to predict the wing weight and its gradient is necessary.

Our previous work<sup>9</sup> validates a design methodology for wing planform optimization with simple estimation of wing weight. We find that if the cost function contains both aerodynamic and structural weight dependencies, the trade-off between these two dependencies will lead to a useful design. However, this raises the question of how to properly integrate these dependencies together. One practical way to solve the relative importance of aerodynamic and structural dependencies is to consider the overall design, such as the maximum range of the aircraft.

In this work, we report improvements in the estimation of wing weight, using a new structural weight model that is sensitive to changes of both geometry and aerodynamic load. Because of the coupling between this wing geometry and aerodynamic load, in order to reduce computational time, we extend the adjoint method to calculate the wing weight gradient

---

\*Doctoral Candidate, AIAA Member

†Thomas V. Jones Professor of Engineering, Department of Aeronautics and Astronautics, AIAA Member

Copyright © 2003 by the American Institute of Aeronautics and Astronautics, Inc. No copyright is asserted in the United States under Title 17, U.S. Code. The U.S. Government has a royalty-free license to exercise all rights under the copyright claimed herein for Governmental Purposes. All other rights are reserved by the copyright owner.

with respect to planform variations.

We also consider an alternative approach of how to combine the aerodynamic and structural cost functions to cover a broader design range, based on the concept of the ‘‘Pareto front’’. This front represents a set that is optimal in the sense that no improvement can be achieved in one objective component that doesn’t lead to degradation in at least one of the remaining components. Accordingly it extends an optimal solution from a single objective function to a multiple objective function, hence broadening the range of design options.

### Mathematical formulation

In this work the equations of steady flow

$$\frac{\partial}{\partial x_i} f_i(w) = 0$$

where  $w$  is the solution vector, and  $f_i(w)$  are the flux vectors along the  $x_i$  axis are applied in a fixed computational domain, with coordinates  $\xi_i$ , so that

$$R(w, S) = \frac{\partial}{\partial \xi_i} F_i(w) = \frac{\partial}{\partial \xi_i} S_{ij} f_j(w) = 0$$

where  $S_{ij}$  are the coefficients of the Jacobian matrix of the transformation. Then geometry changes are represented by changes  $\delta S_{ij}$  in the metric coefficients. Suppose one wishes to minimize the cost function of a boundary integral

$$I = \int_{\mathcal{B}} \mathcal{M}(w, S) d\mathcal{B}_\xi + \int_{\mathcal{B}} \mathcal{N}(w, S) d\mathcal{B}_\xi$$

where the integral of  $\mathcal{M}(w, S)$  could be an aerodynamic cost function, e.g. drag coefficient, and the integral of  $\mathcal{N}(w, S)$  could be a structural cost function, e.g. wing weight. Then one can augment the cost function through Lagrange multiplier  $\psi$  as

$$I = \int_{\mathcal{B}} \mathcal{M}(w, S) d\mathcal{B}_\xi + \int_{\mathcal{D}} \psi^T \mathcal{R}(w, S) d\mathcal{D}_\xi + \int_{\mathcal{B}} \mathcal{N}(w, S) d\mathcal{B}_\xi$$

A shape variation  $\delta S$  causes a variation

$$\delta I = \int_{\mathcal{B}} \delta \mathcal{M} d\mathcal{B}_\xi + \int_{\mathcal{D}} \psi^T \frac{\partial}{\partial \xi_i} \delta F_i d\mathcal{D}_\xi + \int_{\mathcal{B}} \delta \mathcal{N} d\mathcal{B}_\xi,$$

The second term can be integrated by parts to give

$$\int_{\mathcal{B}} n_i \psi^T \delta F_i d\mathcal{B}_\xi - \int_{\mathcal{D}} \frac{\partial \psi^T}{\partial \xi_i} \delta F_i d\mathcal{D}_\xi.$$

Now, choosing  $\psi$  to satisfy the adjoint equation

$$(S_{ij} \frac{\partial f_j}{\partial w})^T \frac{\partial \psi}{\partial \xi_i} = 0 \quad (1)$$

with appropriate boundary conditions

$$n_i \psi^T S_{ij} f_j = \mathcal{M}_w + \mathcal{N}_w, \quad (2)$$

where

$$\mathcal{M}_w = \frac{\partial \mathcal{M}}{\partial w}, \text{ and } \mathcal{N}_w = \frac{\partial \mathcal{N}}{\partial w},$$

the explicit dependence on  $\delta w$  is eliminated, allowing the cost variations to be expressed in terms of  $\delta S$  and the adjoint solution, and hence finally in terms of the change  $\delta \mathcal{F}$  in a function  $\mathcal{F}(\xi)$  defining the shape.

Thus one obtains

$$\delta I = \int \mathcal{G} \delta \mathcal{F} d\xi = \langle \mathcal{G}, \delta \mathcal{F} \rangle$$

where  $\mathcal{G}$  is the infinite dimensional gradient (Frechet derivative) at the cost of one flow and one adjoint solution. Then one can make an improvement by setting

$$\delta \mathcal{F} = -\lambda \mathcal{G}$$

In fact the gradient  $\mathcal{G}$  is generally of a lower smoothness class than the shape  $\mathcal{F}$ . Hence it is important to restore the smoothness. This may be effected by passing to a weighted Sobolev inner product of the form

$$\langle u, v \rangle = \int (uv + \epsilon \frac{\partial u}{\partial \xi} \frac{\partial v}{\partial \xi}) d\xi$$

This is equivalent to replacing  $\mathcal{G}$  by  $\bar{\mathcal{G}}$ , where in one dimension

$$\bar{\mathcal{G}} - \frac{\partial}{\partial \xi} \bar{\mathcal{G}} \frac{\partial \bar{\mathcal{G}}}{\partial \xi} = \mathcal{G}, \quad \bar{\mathcal{G}} = \text{zero at end points}$$

and making a shape change  $\delta \mathcal{F} = -\lambda \bar{\mathcal{G}}$ .

### Implementation

#### Planform design variables

In this work, we model the wing of interest using six planform variables: root chord ( $c_1$ ), mid-span chord ( $c_2$ ), tip chord ( $c_3$ ), span ( $b$ ), sweepback ( $\Lambda$ ), and wing thickness ratio ( $t$ ), as shown in figure 1. This choice of

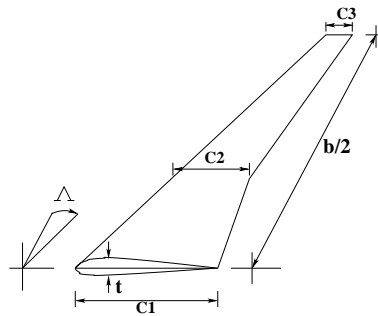


**Fig. 1 Modeled wing governed by six planform variables; root chord ( $c_1$ ), mid-span chord ( $c_2$ ), tip chord ( $c_3$ ), span ( $b$ ), and sweepback ( $\Lambda$ ), wing thickness ratio ( $t$ ).**

design parameters will lead to an optimum wing shape that will not require an extensive structural analysis and can be manufactured effectively.

### Cost function for planform design

In order to design a high performance transonic wing, which will lead to a desired pressure distribution, and still maintain a realistic shape, the natural choice is to set

$$I = \alpha_1 C_D + \alpha_2 \frac{1}{2} \int_{\mathcal{B}} (p - p_d)^2 dS + \alpha_3 C_W \quad (3)$$

with

$$C_W \equiv \frac{\mathcal{W}_{wing}}{q_\infty S_{ref}} \quad (4)$$

where

$C_D$	=	drag coefficient,
$C_W$	=	normalized wing structural weight,
$p$	=	current surface pressure,
$p_d$	=	desired pressure,
$q_\infty$	=	dynamic pressure,
$S_{ref}$	=	reference area,
$\mathcal{W}_{wing}$	=	wing structural weight, and
$\alpha_1, \alpha_2, \alpha_3$	=	weighting parameters for drag, inverse design, and structural weight respectively.

The constant  $\alpha_2$  is introduced to provide the designer some control over the pressure distribution.

### Structural weight model

To estimate  $\mathcal{W}_{wing}$ , a realistic model should account for both planform geometry and wing loading, but it should be simplified enough that we can express it as an analytical function.

An analytical model to estimate the minimal material to resist material and buckling failures has been developed by Wakayama.<sup>10</sup> When shear and buckling effects are small, they may be neglected, resulting in a simplified model developed by Kroo.<sup>11</sup> In this paper, we follow the analysis developed by Kroo.

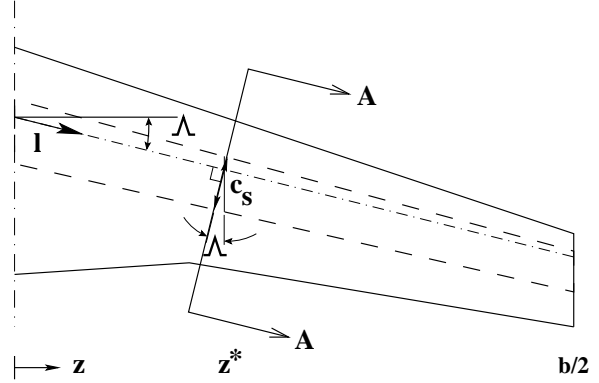
The wing structure is modeled by a structure box, whose major structural material is the box skin. The skin thickness ( $t_s$ ) varies along the span and resists the bending moment caused by the wing lift. Then, the structural wing weight can be calculated based on material of the skin.

Consider a box structure of a swept wing whose quarter-chord swept is  $\Lambda$  and its cross-section A-A as shown in figures 2. The skin thickness  $t_s$ , structure box chord  $c_s$ , and overall thickness  $t$  vary along the span. The maximum normal stress from the bending moment at a section  $Z^*$  is

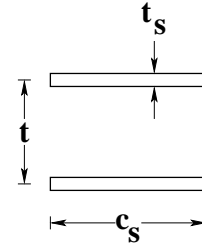
$$\sigma = \frac{M(z^*)}{t t_s c_s}$$

The corresponding wing structural weight is

$$\begin{aligned} \mathcal{W}_{wing} &\propto \int_{\text{structural span}} \frac{M}{t} dl \\ &= 2 \frac{\rho_{mat} g}{\sigma \cos(\Lambda)} \int_{-\frac{b}{2}}^{\frac{b}{2}} \frac{M(z^*)}{t(z^*)} dz^* \end{aligned}$$



a) swept wing planform



b) section A-A

**Fig. 2** Structural model for a swept wing

$$= 4 \frac{\rho_{mat} g}{\sigma \cos(\Lambda)} \int_0^{\frac{b}{2}} \frac{M(z^*)}{t(z^*)} dz^*,$$

and

$$C_W = \frac{\beta}{\cos(\Lambda)} \int_0^{\frac{b}{2}} \frac{M(z^*)}{t(z^*)} dz^*, \quad (5)$$

where

$$\beta = \frac{4 \rho_{mat} g}{\sigma q_\infty S_{ref}},$$

$\rho_{mat}$  is the material density, and  $g$  is the gravitational constant.

The bending moment can be calculated by integrating pressure toward the wing tip.

$$\begin{aligned} M(z^*) &= - \int_{z^*}^{\frac{b}{2}} \frac{p(x, z)(z - z^*)}{\cos(\Lambda)} dA \\ &= - \int_{z^*}^{\frac{b}{2}} \oint_{\text{wing}} \frac{p(x, z)(z - z^*)}{\cos(\Lambda)} dx dz \end{aligned}$$

Thus

$$C_W = \frac{-\beta}{\cos(\Lambda)^2} \int_0^{\frac{b}{2}} \int_{z^*}^{\frac{b}{2}} \oint_{\text{wing}} \frac{p(x, z)(z - z^*)}{t(z^*)} dx dz dz^* \quad (6)$$

To form the corresponding adjoint boundary condition (2),  $C_W$  must be expressed as  $\int_{\mathcal{B}} d\mathcal{B}_\xi$  in the computational domain, or  $\iint dx dz$  in a physical domain to match the boundary term of (2).

To switch the order of integral of (6), introduce a Heaviside function

$$H(z - z^*) = \begin{cases} 0, & z < z^* \\ 1, & z > z^* \end{cases}$$

Then (6) can be rewritten as

$$C_W = \frac{-\beta}{\cos(\Lambda)^2} \cdot \int_0^{\frac{b}{2}} \int_0^{\frac{b}{2}} \oint_{wing} \frac{p(x, z)H(z - z^*)(z - z^*)}{t(z^*)} dx dz dz^* \quad (7)$$

$$= \frac{-\beta}{\cos(\Lambda)^2} \int_0^{\frac{b}{2}} \oint_{wing} p(x, z)K(z) dx dz,$$

where

$$K(z) = \int_0^{\frac{b}{2}} \frac{H(z - z^*)(z - z^*)}{t(z^*)} dz^*$$

$$= \int_0^z \frac{z - z^*}{t(z^*)} dz^*$$

In the computational domain,

$$C_W = \frac{-\beta}{\cos(\Lambda)^2} \oint_B p(\xi_1, \xi_3)K(\xi_3)S_{22}d\xi_1d\xi_3, \quad (8)$$

and  $K(\xi_3)$  is a one-to-one mapping of  $K(z)$ .

### Adjoint boundary condition for the structural weight

For simplicity, it is assumed that the portion of the boundary that undergoes shape modifications is restricted to the coordinate  $\xi_2 = 0$ . Then (2) may be simplified by incorporating the conditions

$$n_1 = n_3 = 0, \quad n_2 = 1 \quad \text{and} \quad d\mathcal{B}_\xi = d\xi_1d\xi_3,$$

so that the only variation  $\delta F_2$  needs to be considered at the wall boundary. Moreover, the condition that there is no flow through the wall boundary at  $\xi_2 = 0$  is equivalent to

$$U_2 = 0,$$

and

$$\delta U_2 = 0$$

when the boundary shape is modified. Consequently,

$$\delta F_2 = \delta p \begin{Bmatrix} 0 \\ S_{21} \\ S_{22} \\ S_{23} \\ 0 \end{Bmatrix} + p \begin{Bmatrix} 0 \\ \delta S_{21} \\ \delta S_{22} \\ \delta S_{23} \\ 0 \end{Bmatrix}. \quad (9)$$

The variation of  $C_W$  is

$$\delta C_W = -\beta \oint_B \delta p \frac{KS_{22}}{\cos(\Lambda)^2} + p\delta \left( \frac{KS_{22}}{\cos(\Lambda)^2} \right) d\xi_1d\xi_3, \quad (10)$$

Since  $\delta F_2$  and  $\delta C_W$  depend only on the pressure, it allows a complete cancellation of dependency of the boundary integral on  $\delta p$ , and the adjoint boundary condition reduces to

$$\psi_2 S_{21} + \psi_3 S_{22} + \psi_4 S_{23} = \frac{-\beta}{\cos(\Lambda)^2} K S_{22} \quad (11)$$

### Adjustment of the adjoint boundary condition for a design with fixed $C_L$

A typical design problem is to find an optimum wing shape, while maintaining constant lift. A practical way to maintain the lift is to allow the angle of attack to adjust at each design cycle. In such a case the variation of the cost function needs to include a variation from the change of angle of attack.

If

$$I = C_W,$$

then

$$\delta I = \tilde{\delta} C_w + \frac{\partial C_W}{\partial \alpha} \delta \alpha \quad (12)$$

where  $\tilde{\delta}$  refers to variations independent of changes in  $\alpha$ . For fixed lift,

$$\begin{aligned} \delta C_L &= 0 \\ &= \delta [C_N \cos(\alpha) - C_A \sin(\alpha)] \\ &= \tilde{\delta} C_N \cos(\alpha) - \tilde{\delta} C_A \sin(\alpha) \\ &\quad + \left[ \frac{\partial C_N}{\partial \alpha} \cos(\alpha) - \frac{\partial C_A}{\partial \alpha} \sin(\alpha) \right] \delta \alpha \\ &\quad + [-C_N \sin(\alpha) - C_A \cos(\alpha)] \delta \alpha, \end{aligned} \quad (13)$$

leaving

$$\begin{aligned} \delta \alpha &= \frac{-\tilde{\delta} C_N \cos(\alpha) + \tilde{\delta} C_A \sin(\alpha)}{-CD + \frac{\partial C_N}{\partial \alpha} \cos(\alpha) - \frac{\partial C_A}{\partial \alpha} \sin(\alpha)} \\ &= \frac{-\tilde{\delta} C_N \cos(\alpha) + \tilde{\delta} C_A \sin(\alpha)}{\frac{\partial C_L}{\partial \alpha}} \end{aligned} \quad (14)$$

Combining (12) and (14), and using

$$\frac{\frac{\partial C_W}{\partial \alpha}}{\frac{\partial C_L}{\partial \alpha}} = \frac{\partial C_W}{\partial C_L},$$

(12) becomes

$$\delta I = \tilde{\delta} C_w + \frac{\partial C_W}{\partial C_L} \left( -\tilde{\delta} C_N \cos(\alpha) + \tilde{\delta} C_A \sin(\alpha) \right) \quad (15)$$

To calculate  $\frac{\partial C_W}{\partial C_L}$ , an outer iteration needs to be incorporated with the flow solver which changes  $\alpha$ .

To express the corresponding adjoint boundary condition, recall

$$C_N = \frac{-1}{q_\infty S_{ref}} \int_B p S_{22} d\xi_1 d\xi_3 \quad (16)$$

$$C_A = \frac{-1}{q_\infty S_{ref}} \int_B p S_{21} d\xi_1 d\xi_3 \quad (17)$$

Following the procedure outlined in the previous section, equations (15), (16), and (17) can be combined with the variation of the flow equations and equation (11) will be modified to

$$\begin{aligned} \psi_2 S_{21} + \psi_3 S_{22} + \psi_4 S_{23} = \\ \frac{-\beta}{\cos(\Lambda)^2} K S_{22} - \gamma \sin(\alpha) S_{21} + \gamma \cos(\alpha) S_{22} \end{aligned} \quad (18)$$

where  $\gamma = \frac{\frac{\partial C_W}{\partial C_L}}{q_\infty S_{ref}}$ .

## Gradient calculation for planform variables

Gradient information can be computed using a variety of approaches such as the finite-difference method, the complex step method,<sup>12</sup> and the automatic differentiation.<sup>13</sup> Unfortunately, their computational cost is still proportional to the number of design variables in the problem. In an optimum transonic wing design, suppose one chooses mesh points on a wing surface as the design variables, which is on the order of 1000 or more; it is impractical to calculate the gradient using the methods mentioned earlier. In our planform optimization, the design variables are points on the wing surface plus the planform variables. To evaluate the aerodynamic and structural gradients with respect to the planform variables, since the number of planform variables (six in this study) is far less than that of the surface optimization, one could calculate the gradient by the finite-difference method, the complex step method or the automatic differentiation. However, the cost for the gradient calculation will be six times higher. A more efficient approach is to follow the adjoint formulation.

Consider the variation of the cost function (3)

$$\delta I = \int_{\mathcal{B}} (\delta \mathcal{M} + \delta \mathcal{N}) d\mathcal{B}_\xi + \int_{\mathcal{D}} \psi^T \delta R d\mathcal{D}_\xi$$

This can be split as

$$\delta I = [I_w]_I \delta w + \delta I_{II}$$

with

$$\delta \mathcal{M} = [\mathcal{M}_w]_I \delta w + \delta \mathcal{M}_{II}$$

and

$$\delta \mathcal{N} = [\mathcal{N}_w]_I \delta w + \delta \mathcal{N}_{II}$$

where the subscripts  $I$  and  $II$  are used to distinguish between the contributions associated with variation of the flow solution  $\delta w$  and those associated with the metric variations  $\delta S$ . Thus  $[\mathcal{M}_w]_I$  represents  $\frac{\partial \mathcal{M}}{\partial w}$  with the metrics fixed. Note that  $\delta R$  is intentionally kept unsplit for programming purposes. If one chooses  $\psi$  as  $\psi^*$ , where  $\psi^*$  satisfies

$$(S_{ij} \frac{\partial f_j}{\partial w})^T \frac{\partial \psi^*}{\partial \xi_i} = 0,$$

then

$$\begin{aligned} \delta I(w, S) &= \delta I(S) \\ &= \int_{\mathcal{B}} (\delta \mathcal{M}_{II} + \delta \mathcal{N}_{II}) d\mathcal{B}_\xi + \int_{\mathcal{D}} \psi^{*T} \delta R d\mathcal{D}_\xi \\ &\approx \sum_{\mathcal{B}} (\delta \mathcal{M}_{II} + \delta \mathcal{N}_{II}) \Delta \mathcal{B} + \sum_{\mathcal{D}} \psi^{*T} \Delta \bar{R} \\ &\approx \sum_{\mathcal{B}} (\delta \mathcal{M}_{II} + \delta \mathcal{N}_{II}) \Delta \mathcal{B} \\ &+ \sum_{\mathcal{D}} \psi^{*T} (\bar{R}|_{S+\delta S} - \bar{R}|_S), \end{aligned}$$

where  $\bar{R}|_S$  and  $\bar{R}|_{S+\delta S}$  are volume weighted residuals calculated at the original mesh and at the mesh perturbed in the design direction.

Provided that  $\psi^*$  has already been calculated and  $\bar{R}$  can be easily calculated, the gradient of the planform variables can be computed effectively by first perturbing all the mesh points along the direction of interest. For example, to calculate the gradient with respect to the sweepback, move all the points on the wing surface as if the wing were pushed backward and also move all other associated points in the computational domain to match the new location of points on the wing. Then re-calculate the residual value and subtract the previous residual value from the new value to form  $\Delta \bar{R}$ . Finally, to calculate the planform gradient, multiply  $\Delta \bar{R}$  by the costate vector and add the contribution from the boundary terms.

This way of calculating the planform gradient exploits the full benefit of knowing the value of adjoint variables  $\psi^*$  with no extra cost of flow or adjoint calculations.

## Choice of weighting constants

### Maximizing range of the aircraft

The choice of  $\alpha_1$  and  $\alpha_3$  greatly affects the optimum shape. If  $\frac{\alpha_3}{\alpha_1}$  is high enough, the optimum shape will have lower  $C_D$  and higher  $C_W$  than another optimum shape with lower  $\frac{\alpha_3}{\alpha_1}$  value.

Leoviriyakit and Jameson<sup>9</sup> propose an intuitive choice of  $\alpha_1$  and  $\alpha_3$  by equating a problem of maximizing range of an aircraft to a problem of minimizing the cost function

$$I = C_D + \frac{\alpha_3}{\alpha_1} C_W.$$

If the simplified Breguet range equation can be expressed as

$$R = \frac{V L}{C D} \log \frac{W_1}{W_2}$$

where  $C$  is specific fuel consumption,  $D$  is drag,  $L$  is lift,  $R$  is range,  $V$  is aircraft velocity,  $W_1$  is take off weight, and  $W_2$  is landing weight, then choosing

$$\frac{\alpha_3}{\alpha_1} = \frac{C_D}{C_{W_2} \log \frac{C_{W_1}}{C_{W_2}}}, \quad (19)$$

corresponds to maximizing the range of the aircraft.

### Pareto Front

In order to present the designer with a wider range of choices, the problem of optimizing both drag and weight can be treated as a multi-objective optimization problem. In this sense one may also view the problem as a “game”, where one player tries to minimize  $C_D$  and the other tries to minimize  $C_W$ . In order to compare the performance of various trial designs, designated by the symbol  $X$  in figure 3, they

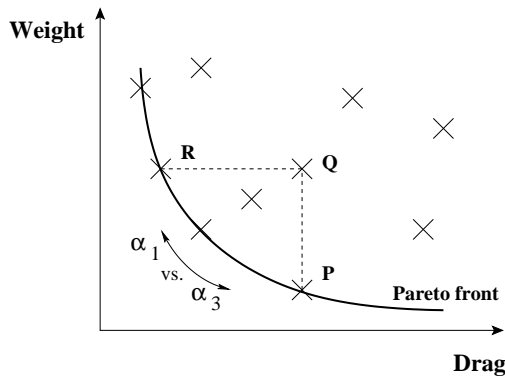


Fig. 3 Cooperative game strategy with drag and weight as players

may be ranked for both drag and weight. A design is undominated if it is impossible either to reduce the drag for the same weight or to reduce the weight for the same drag. Any dominated point should be eliminated, leaving a set of undominated points which form the Pareto front. In figure 3, for example, the point Q is dominated by the point P (same drag, less weight) and also the point R (same weight, less drag). So the point Q will be eliminated. The Pareto front can be fit through the points P, R and other dominating points, which may be generated by using an array of different values of  $\alpha_1$  and  $\alpha_3$  in the cost function to compute different optimum shapes. With the aid of the Pareto front the designer will have freedom to pick the most useful design.

### Design cycle

The design cycle starts by first solving the flow field until at least a 4 order of magnitude drop in the residual. The flow solution is then passed to the adjoint solver. Second, the adjoint solver is run to calculate the costate vector. Iteration continues until at least a 4 order of magnitude drop in the residual. The costate vector is passed to the gradient module to evaluate the overall gradient, which combines the aerodynamic and structural parts. The steepest descent method is used with a small step size to guarantee that the solution will converge to the optimum point. The design cycle is shown in figure 4.

### Flow solver and adjoint solver

The flow solver and the adjoint solver chosen in this work are codes developed by Jameson.<sup>3,4,14,15</sup> The flow solver solves the three dimensional Euler equations, by employing the JST scheme, together with a multi-step time stepping scheme. Rapid convergence to a steady state is achieved via variable local time steps, residual averaging, and a full approximation multi-grid scheme. The adjoint solver solves the corresponding adjoint equations using similar techniques to those of the flow solver. In fact much of the software is shared by the flow solver and adjoint solver.

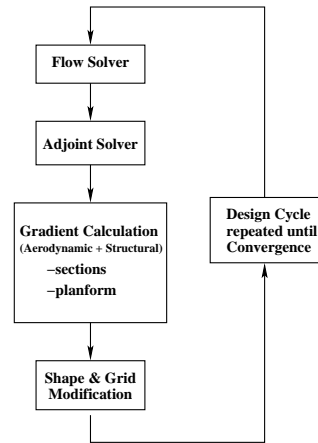


Fig. 4 Design cycle

## Results

### Validation of aerodynamic and structural gradients with respect to planform variables

To verify the accuracy of the aerodynamic and structural gradients with respect to planform variables calculated by employing the adjoint method, we compare the planform gradients using adjoint and finite-difference methods. For the purpose of comparison, calculations are done at a fixed angle of attack to eliminate the effect of pitch variation on the gradient. The case chosen is the Boeing 747 wing fuselage combination at Mach 0.87, and wing angle of attack 2.3 degrees. The computational mesh is shown in figure 5.

The gradients with respect to the planform variables are calculated using both the adjoint and the finite-difference methods. A forward differencing technique is used for the finite-difference method with a moderate step size of 0.1% of planform variables to achieve both small discretization error and small cancellation error. The flow and adjoint solvers are run until both solutions are fully converged.

To verify the result more generally, different geometries are used in this comparison. Each new geometry is generated sequentially by allowing section changes of the current geometry. Figures 6 and 7 show the planform gradient comparison where the cost functions are  $C_D$  and  $C_W$  respectively. It can be seen that the results from both adjoint and finite difference methods match each other very well, independent of the geometry. This result indicates that the adjoint method provides an accurate planform gradient while reducing the computational cost by a factor of six.

The effect of the step size for the mesh perturbations used in the gradient calculation has been studied by Leoviriyakit and Jameson.<sup>9</sup> The results indicate that the step size almost has no effect on the adjoint gradient, showing an additional advantage of the adjoint gradient over the finite difference gradient. Similar results have been indicated by Kim et. al.<sup>16</sup>

## Redesign of the Boeing 747 wing

We present a result to show that the optimization can successfully trade planform parameters. We also demonstrate how to apply strategy game theory to the gradient based optimization.

Here, the case chosen is the Boeing 747 wing fuselage combination at Mach 0.87 and a lift coefficient  $C_L = 0.42$ . The computational mesh is shown in figure 5.

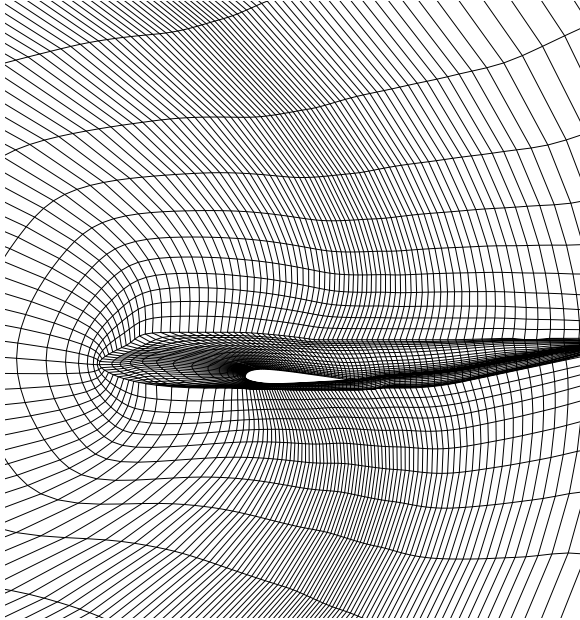


**Fig. 5** Computational grid of the B747 wing fuselage

In this test case, the Mach number is slightly higher than the current normal cruising Mach number of 0.85. We allowed section changes together with variations of sweep angle, span length, chords, and section thickness. Figure 8 shows an optimization with fixed planform. Here the drag was reduced from 107.7 counts to 93.9 counts in seventeen design iterations with relatively small changes in the section shape, while the structural weight is maintained constant at  $C_W = 0.0455$ .

Figure 9 shows the effect of allowing changes in sweepback, span length, chords at root, break, and tip locations, and section thickness. In our previous work, the section thickness was held constant. However, in order to fully exploit the planform optimization, it is important to allow thickness variations, since an increase in thickness will allow an increase in span for the same weight. At the same time the section optimization can prevent an increase in shock drag. The parameter  $\alpha_3$  was chosen according to formula (19) such that the cost function corresponds to maximizing the range of the aircraft. Here in nineteen design iterations the drag was reduced from 107.7 counts to 87.2 counts. The further reduction in drag is the result of the increase in span from 191.5 ft to 205.7 ft, which reduces the induced drag. The redesigned geom-

etry also has a lower sweep angle and a thicker wing section in the inboard part of the wing, which both reduce the structural weight. The optimized geometry is shown in figure 10. Overall, the re-design with variation planform gives improvements in both aerodynamic performance and structural weight, compared to the previous optimization with a fixed planform.

Figure 11 shows the effect of weighting parameters ( $\alpha_1, \alpha_3$ ) on the optimal design. Here, each point corresponds to an optimal shape for one specific  $(\alpha_1, \alpha_3)$ . The cost function now becomes a multiple objective function, measured in terms of drag and wing weight. By varying  $\alpha_1$  and  $\alpha_3$ , we can capture the Pareto front. Since all points on the Pareto front are acceptable solutions, any further choice to select the final design depends on the nature of the problem and several other factors. Also notice that the optimum shape that corresponds to the optimal Breguet range is a particular point on the Pareto front.

## Conclusion

The feasibility of an aerodynamic design methodology for planform optimization has been demonstrated. To realize meaningful designs, a model for the structural weight is included in the design cost function. A more realistic model for the structural weight, which is sensitive to both planform variations and wing loading, is included in the design cost function to provide a meaningful design. The results of optimizing the wing-fuselage of a commercial transonic transport aircraft has highlighted the importance of the structural weight model. It is the trade-off between the structural cost function and the aerodynamic cost function that prevents an unrealistic result and leads to a useful design. Hence a good structural model can be critical in aerodynamic planform optimization.

## Acknowledgment

This work has benefited greatly from the support of the Air Force Office of Science Research under grant No. AF F49620-98-1-2002.

## References

- <sup>1</sup>A. Jameson. Aerodynamic design via control theory. *Journal of Scientific Computing*, 3:233–260, 1988.
- <sup>2</sup>A. Jameson. Computational aerodynamics for aircraft design. *Science*, 245:361–371, 1989.
- <sup>3</sup>A. Jameson, L. Martinelli, and N. A. Pierce. Optimum aerodynamic design using the Navier-Stokes equations. *Theoretical and Computational Fluid Dynamics*, 10:213–237, 1998.
- <sup>4</sup>A. Jameson. A perspective on computational algorithms for aerodynamic analysis and design. *Progress in Aerospace Sciences*, 37:197–243, 2001.
- <sup>5</sup>A. Jameson and L. Martinelli. Aerodynamic shape optimization techniques based on control theory. Technical report, CIME (International Mathematical Summer Center), Martina Franca, Italy, 1999.
- <sup>6</sup>J. C. Vassberg and A. Jameson. Computational fluid dynamics for aerodynamic design: Its current and future impact. *AIAA paper 2001-0538*, AIAA 39th Aerospace Sciences Meeting & Exhibit, Reno, NV, January 2001.



<sup>7</sup>J. C. Vassberg and A. Jameson. Aerodynamic shape optimization of a reno race plane. *International Journal of Vehicle Design*, 28:318–338, 2002.

<sup>8</sup>S. Kim, J. J. Alonso, and A. Jameson. Design optimization of high-lift configurations using a viscous continuous adjoint method. *AIAA paper 2002-0844*, AIAA 40th Aerospace Sciences Meeting & Exhibit, Reno, NV, January 2002.

<sup>9</sup>K. Leoviriyakit and A. Jameson. Aerodynamic shape optimization of wings including planform variables. *AIAA paper 2003-0210*, 41st Aerospace Sciences Meeting & Exhibit, Reno, Nevada, January 2003.

<sup>10</sup>S. Wakayama. Lifting surface design using multidisciplinary optimization. Technical report, Stanford University Doctoral Dissertation, Stanford, CA, 1994.

<sup>11</sup>I. M. Kroo. Design and analysis of optimally-loaded lifting systems. *AIAA paper 1984-2507*, October 1984.

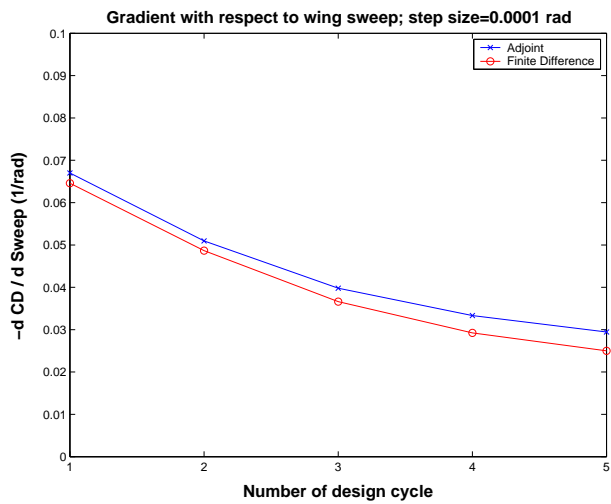
<sup>12</sup>J. R. R. A. Martins, I. M. Kroo, and J. J. Alonso. An automated method for sensitivity analysis using complex variables. *AIAA paper 2000-0689*, 38th Aerospace Sciences Meeting, Reno, Nevada, January 2000.

<sup>13</sup>C. Bischof, A. Carle, G. Corliss, A. Griewank, and P. Holland. Generating derivative codes from Fortran programs. *Internal report MCS-P263-0991*, Computer Science Division, Argonne National Laboratory and Center of Research on Parallel Computation, Rice University, 1991.

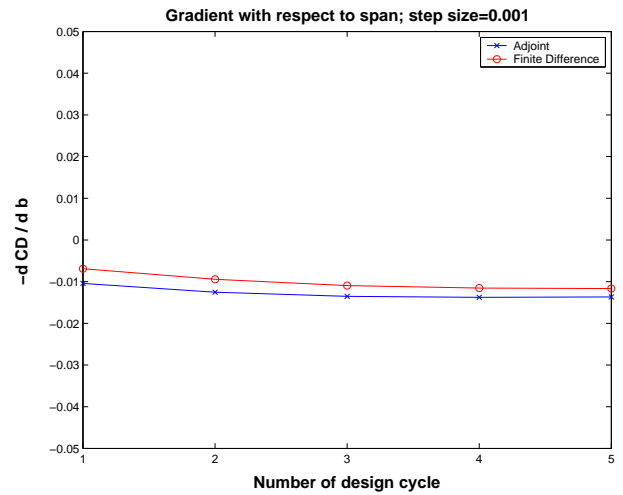
<sup>14</sup>A. Jameson. Analysis and design of numerical schemes for gas dynamics 1, artificial diffusion, upwind biasing, limiters and their effect on multigrid convergence. *Int. J. of Comp. Fluid Dyn.*, 4:171–218, 1995.

<sup>15</sup>A. Jameson. Analysis and design of numerical schemes for gas dynamics 2, artificial diffusion and discrete shock structure. *Int. J. of Comp. Fluid Dyn.*, 5:1–38, 1995.

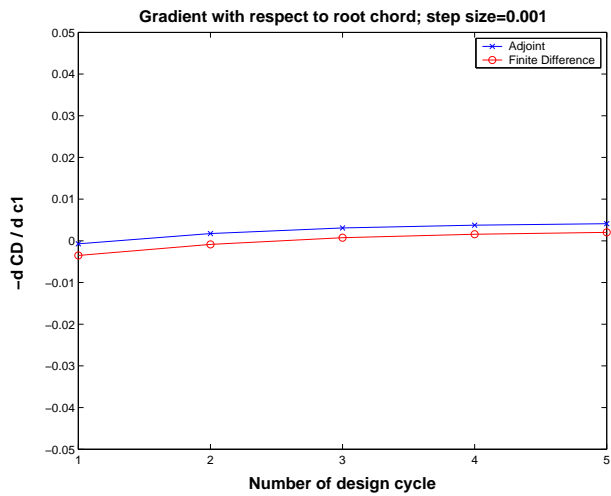
<sup>16</sup>S. Kim, J. J. Alonso, and A. Jameson. A gradient accuracy study for the adjoint-based Navier-Stokes design method. *AIAA paper 1999-0299*, 37th Aerospace Science Meeting & Exhibit, Reno, Nevada, January 1999.



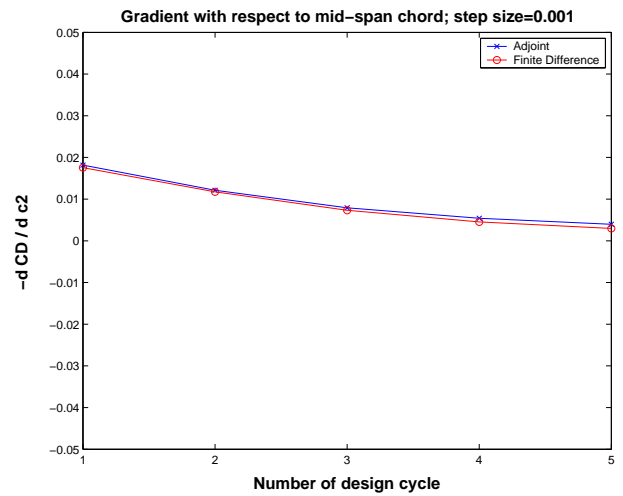
a) Sweepback Angle  $\Lambda$ .



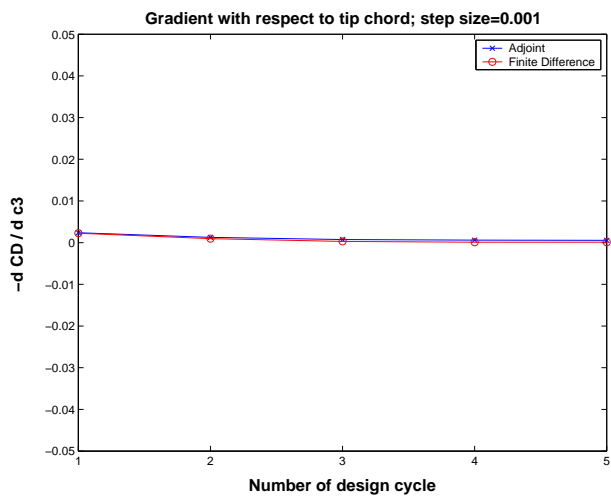
b) Span  $b$ .



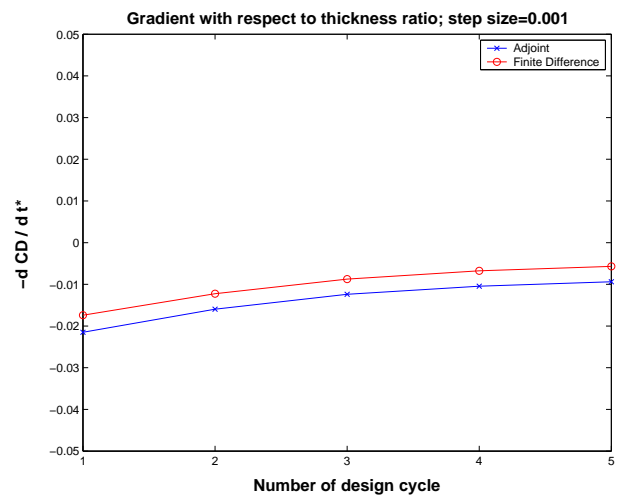
c) Root chord  $c_1$ .



d) Mid-span chord  $c_2$ .



e) Tip chord  $c_3$ .

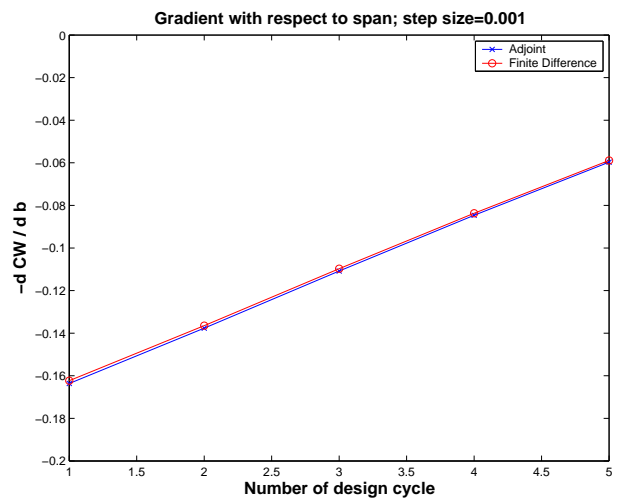


f) Wing thickness ratio  $t$ .

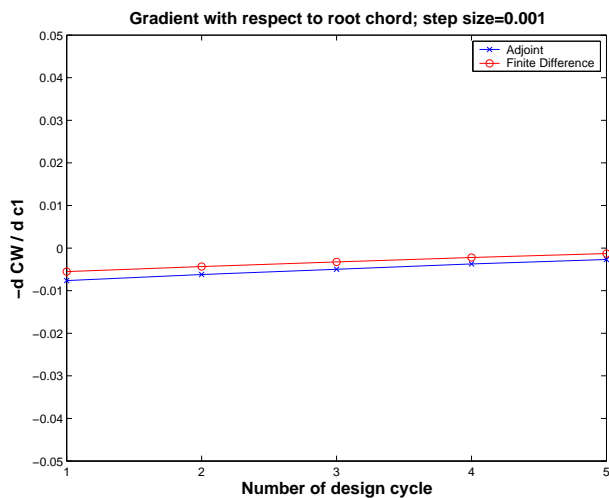
Fig. 6 Comparison between adjoint and finite-difference aerodynamic-gradients with respect to planform variables. Test case: Boeing 747, wing-body configuration,  $M_\infty=.87$ , fixed  $\alpha=2.3$  degrees.



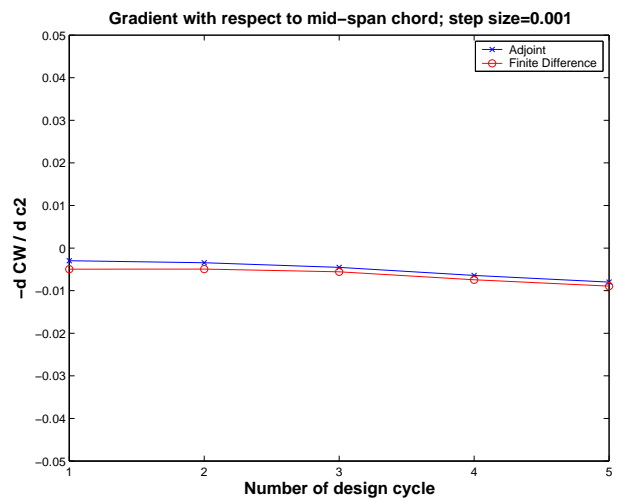
a) Sweepback Angle  $\Lambda$ .



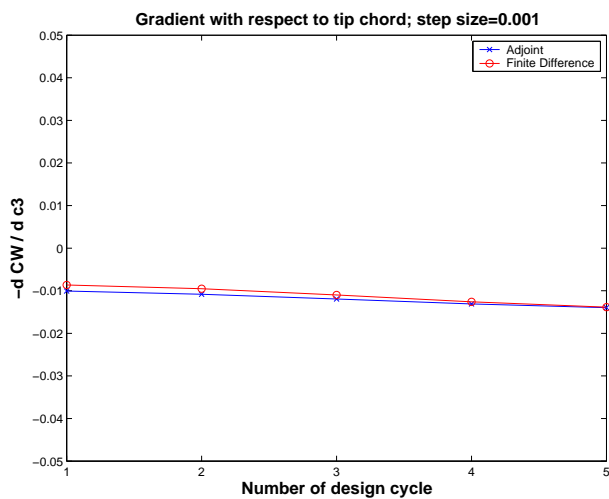
b) Span  $b$ .



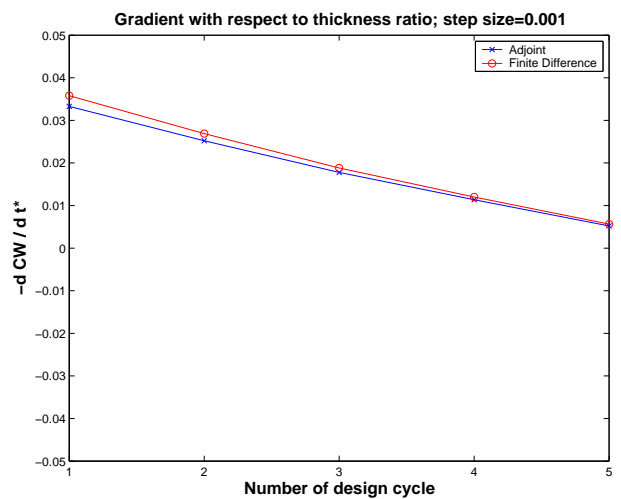
c) Root chord  $c_1$ .



d) Mid-span chord  $c_2$ .



e) Tip chord  $c_3$ .



f) Wing thickness ratio  $t$ .

Fig. 7 Comparison between adjoint and finite-difference structural-gradients with respect to planform variables. Test case: Boeing 747, wing-body configuration,  $M_\infty=.87$ , fixed  $\alpha=2.3$  degrees.

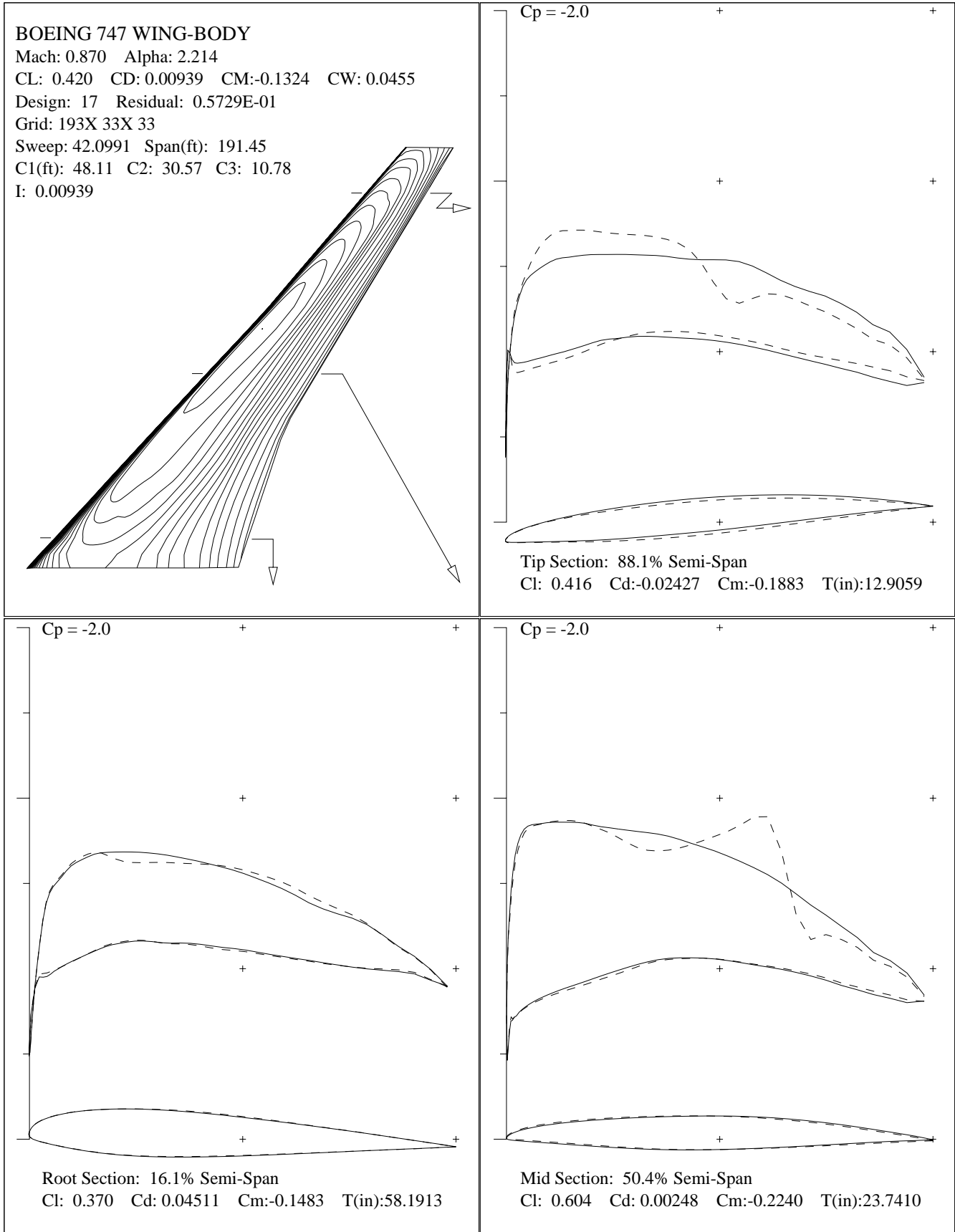


**Fig. 8 Redesign of Boeing 747, using only section modification. Dash line represents shape and pressure distribution of the initial configuration. Solid line represents those of the redesigned configuration.**

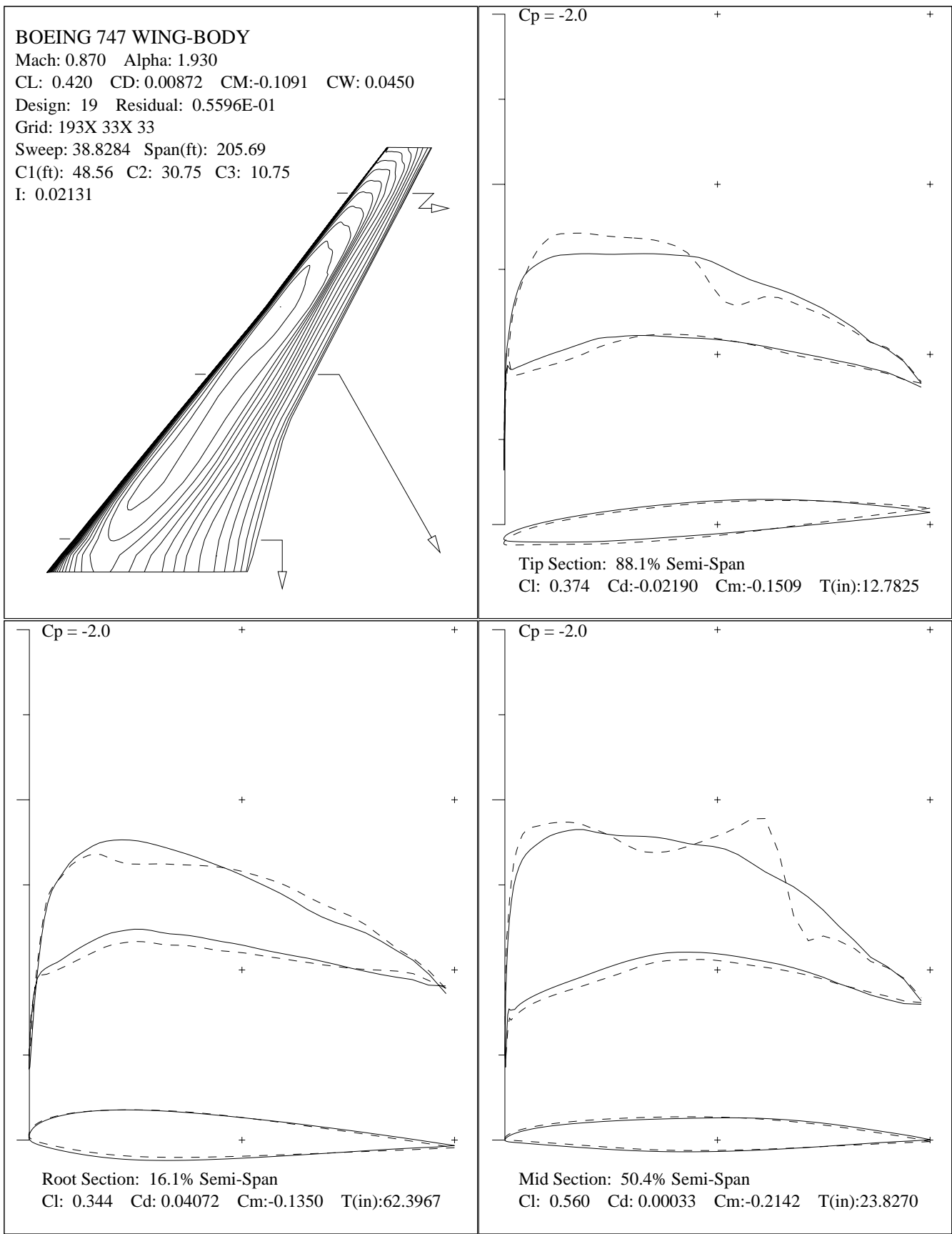


**Fig. 9 Redesign of Boeing 747, using section and planform modifications. Dash line represents shape and pressure distribution of the initial configuration. Solid line represents those of the redesigned configuration.**

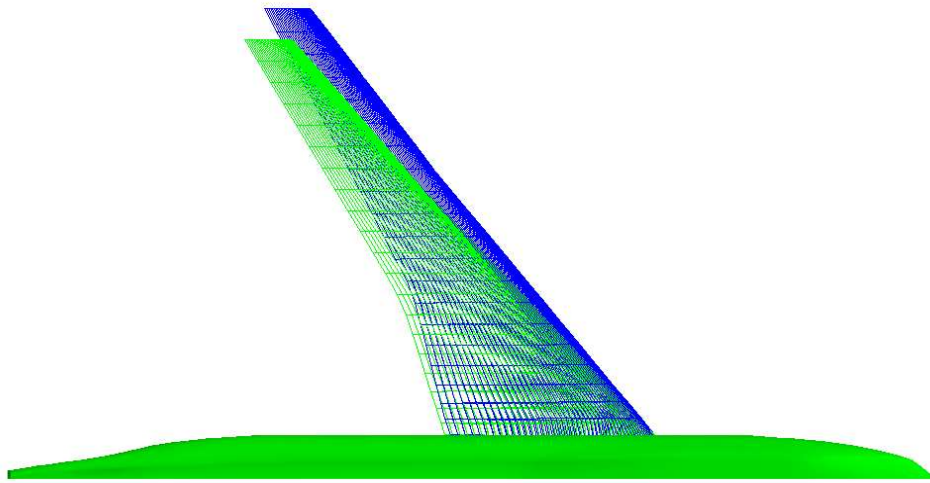


Fig. 10 Superposition of the baseline and the optimized section-and-planform geometries of Boeing 747. The redesigned geometry has a longer span and a lower sweep angle.

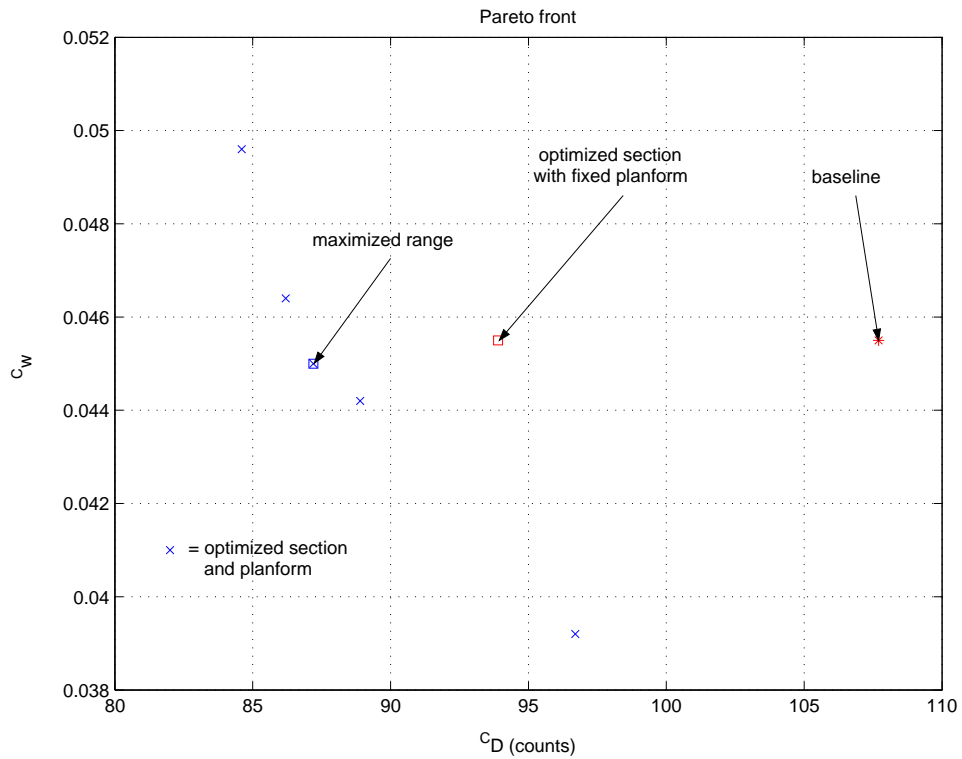


Fig. 11 Pareto front of section and planform modifications